Bioconjugate Chemistry

Article

pubs.acs.org/bc

Sacituzumab Govitecan (IMMU-132), an Anti-Trop-2/SN-38 Antibody−Drug Conjugate: Characterization and Efficacy in Pancreatic, Gastric, and Other Cancers

Thomas M. Cardillo,*[,†] Serengulam V. Govindan,[†] Robert M. Sharkey,[†] Preeti Trisal,[†] Roberto Arrojo,[†] Donglin Liu,[†] Edmund A. Rossi,[†,‡] Chien-Hsing Chang,[†,‡] and David M. Goldenberg*[,†,‡,§]

[†]Immunomedics, Inc., Morris Plains, New Jersey 07950, United States

[‡]IBC Pharmaceuticals, Inc., Morris Plains, New Jersey 07950, United States

[§]Center of Molecular Medicine and Immunology, Garden State Cancer Center, Morris Plains, New Jersey 07950, United States

Supporting Information

ABSTRACT: Sacituzumab govitecan (IMMU-132) is an antibody−drug conjugate (ADC) made from a humanized anti-Trop-2 monoclonal antibody (hRS7) conjugated with the active metabolite of irinotecan, SN-38. In addition to its further characterization, as the clinical utility of IMMU-132 expands to an ever-widening range of Trop-2-expressing solid tumor types, its efficacy in new disease models needs to be explored in a nonclinical setting. Unlike most ADCs that use ultratoxic drugs and stable linkers, IMMU-132 uses a moderately toxic drug with a moderately stable carbonate bond between SN-38 and the linker. Flow cytometry and immunohistochemistry disclosed that Trop-2 is expressed in a wide range of tumor types, including gastric, pancreatic, triple-negative breast (TNBC), colonic, prostate, and lung. While cell-binding experiments reveal no significant differences between IMMU-132 and parental hRS7 antibody, surface plasmon resonance analysis using a Trop-2 CM5 chip shows a significant binding advantage for IMMU-132 over hRS7. The conjugate retained binding to the neonatal receptor, but it lost greater than 60% of the antibody-dependent cell-mediated cytotoxicity activity compared to that of hRS7. Exposure of tumor cells to either free SN-38 or IMMU-132 demonstrated the same signaling pathways, with pJNK1/2 and $p21^{WAF1/Cip1}$ upregulation followed by cleavage of caspases 9, 7, and 3, ultimately leading to poly-ADP-ribose polymerase cleavage and double-stranded DNA breaks. Pharmacokinetics of the intact ADC in mice reveals a mean residence time (MRT) of 15.4 h, while the carrier hRS7 antibody cleared at a similar rate as that of the unconjugated antibody (MRT ∼ 300 h). IMMU-132 treatment of mice bearing human gastric cancer xenografts (17.5 mg/kg; twice weekly × 4 weeks) resulted in significant antitumor effects compared to that of mice treated with a nonspecific control. Clinically relevant dosing schemes of IMMU-132 administered either every other week, weekly, or twice weekly in mice bearing human pancreatic or gastric cancer xenografts demonstrate similar, significant antitumor effects in both models. Current Phase I/II clinical trials (ClinicalTrials.gov, NCT01631552) confirm anticancer activity of IMMU-132 in cancers expressing Trop-2, including gastric and pancreatic cancer patients.

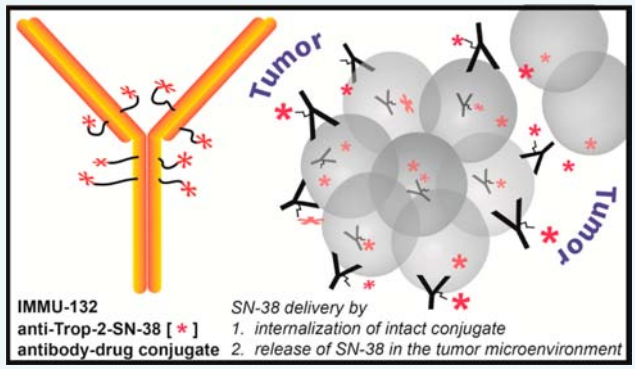

INTRODUCTION

There will be an estimated 22 220 new cases of gastric cancer diagnosed in the United States this year, with a further 10 990 deaths attributed to this disease.[1] While 5 year survival rates are trending upward (currently at 29%), they are still quite low when compared to that of most others, including cancers of the colon, breast, and prostate (65, 90, and 100%, respectively). In fact, among human cancers, only esophageal, liver, lung, and pancreatic have worse 5 year survival rates. Pancreatic cancer remains the fourth leading cause of all cancer deaths in the U.S., with a 5 year survival rate of only 6%.[1] It is clear from such grim statistics for gastric and pancreatic cancer that new therapeutic approaches are needed.

Trop-2 is a 45 kDa glycoprotein that belongs to the *TACSTD* gene family, specifically *TACSTD2*.[2] Overexpression of this transmembrane protein on many different epithelial cancers has been linked to an overall poor prognosis.[3−9] Trop-2 is essential for anchorage-independent cell growth and tumorigenesis.[10,11] It functions as a calcium signal transducer that requires an intact cytoplasmic tail that is phosphorylated by protein kinase C.[12−14] Pro-growth signaling associated with Trop-2 includes NF-κB, cyclin D1, and ERK.[15,16] In pancreatic cancer, Trop-2 overexpression was observed in 55% of patients studied, with a

Received: March 10, 2015
Published: April 27, 2015

DOI: 10.1021/acs.bioconjchem.5b00223
Bioconjugate Chem. 2015, 26, 919−931

positive correlation with metastasis, tumor grade, and poor progression-free survival of patients who underwent surgery with curative intent.[8] Likewise, in gastric cancer, 56% of patients exhibited Trop-2 overexpression on their tumors, which again correlated with shorter disease-free survival and a poorer prognosis in those patients with lymph node involvement of Trop-2-positive tumor cells.[9] Given these characteristics and the fact that Trop-2 is linked to so many intractable cancers, Trop-2 is an attractive target for therapeutic intervention with an antibody−drug conjugate (ADC).

A general paradigm for using an antibody to target a drug to a tumor includes several key features, among them (a) an antigen target that is preferentially expressed on the tumor versus normal tissue, (b) an antibody that has good affinity and is internalized by the tumor cell, and (c) an ultratoxic drug that is coupled stably to the antibody.[17] Along these lines, we developed an antibody, designated RS7-3G11 (RS7), that bound to Trop-2 in a number of solid tumors[14,18,19] with nanomolar affinity[20] and once bound to Trop-2 is internalized by the cell.[21] By immunohistochemistry, Trop-2 is expressed in some normal tissues, although usually at much lower intensities when compared to those in neoplastic tissue, and often is present in regions of the tissues with restricted vascular access.[11] On the basis of these characteristics, RS7 was humanized and conjugated with the active metabolite of irinotecan, 7-ethyl-10-hydroxycamptothecin (SN-38). *In vitro* cytotoxicity in numerous cell lines has found IC_{50} values in the single-digit nanomolar range for SN-38, compared to picomolar range for many of the ultratoxic drugs currently used in ADCs.[20] While the prevailing opinion is to use ultratoxic agents, such as auristatins or maytansines, to make ADCs with only 2−4 drugs per antibody linked stably to the antibody, such agents have a narrow therapeutic window, resulting in renewed efforts to re-engineer ADCs to broaden their therapeutic index.[22] As one approach to diverge from this practice, we conjugated 7 to 8 SN-38 molecules per antibody using a linker that releases SN-38 with half-life of ∼1 day in human serum.[20] It is hypothesized that using a less stable linker allows for SN-38 to be released at the tumor site after the ADC targets the cells, making the drug accessible to surrounding tumor cells and not just cells directly targeted by the ADC. The resulting ADC, hRS7-CL2A-SN-38 (sacituzumab govitecan, or IMMU-132), has shown antitumor activity against a wide range of tumor types.[20] More recently, IMMU-132 has demonstrated significant antitumor activity against a preclinical model of triple negative breast cancer (TNBC).[23] Most importantly, in a current Phase I/II clinical trial, IMMU-132 has shown activity in TNBC patients,[24] thus validating this paradigm shift in ADC chemistry using a less toxic drug and a linker that releases SN-38 over time rather than being totally dependent on internalization of the ADC to achieve activity.

SN-38 is a known topoisomerase-I inhibitor that induces significant damage to a cell's DNA. It mediates the upregulation of early pro-apoptotic proteins, p53 and $p21^{WAF1/Cip1}$, resulting in caspase activation and poly-ADP-ribose polymerase (PARP) cleavage.[25−28] Expression of $p21^{WAF1/Cip1}$ is associated with G_1 arrest of the cell cycle and is thus a hallmark of the intrinsic apoptotic pathway.[29,30] We demonstrated previously that IMMU-132 likewise could mediate the upregulation of early pro-apoptosis signaling events (p53 and $p21^{WAF1/Cip1}$), resulting in PARP cleavage in NSCLC (Calu-3) and pancreatic (BxPC-3) cell lines, consistent with the intrinsic pro-apoptosis signaling pathway.[20]

Herein, we further characterize IMMU-132, with particular attention toward the treatment of solid cancers, especially human gastric and pancreatic tumors. Trop-2 surface expression across a range of solid tumor types is examined and correlated with *in vivo* expression in tumor xenografts. Mechanistic studies further elucidate the intrinsic pro-apoptotic signaling events mediated by IMMU-132, including evidence of increased double-stranded DNA (dsDNA) breaks and later caspase activation. Finally, clinically relevant and nontoxic dosing schemes are compared in gastric and pancreatic carcinoma disease models, testing twice-weekly, weekly, and every other week schedules to ascertain which treatment cycle may be best applied to a clinical setting without loss of efficacy.

RESULTS

Trop-2 Expression Levels in Multiple Solid Tumor Cell Lines. Surface expression of Trop-2 is evident in a variety of human solid tumor lines, including gastric, pancreatic, breast, colon, and lung (Table 1). There is no one tumor type that had higher expression above any other, with variability observed within a given tumor cell type. For example, within gastric adenocarcinomas, Trop-2 levels ranged from very low 494 ± 19 (Hs 746T) to high 246 857 ± 64 651 (NCI-N87) surface molecules per cell.

Table 1. Trop-2 Surface Expression Levels in Various Solid Tumor Lines via FACS Analysis[a]

	no. of surface Trop-2 molecules per cell
Cell Line	mean ± SD
Gastric	
NCI-N87	246 857 ± 64 651
AGS	53 756 ± 23 527
Hs 746T	494 ± 19
Pancreatic	
BxPC-3	493 773 ± 97 779
CFPAC-1	162 871 ± 28 161
Capan-1	157 376 ± 36 976
HPAF-II	115 533 ± 28 627
Breast (TN)	
MDA-MB-468	301 603 ± 29 470
HCC38	181 488 ± 69 351
HCC1806	91 403 ± 20 817
MDA-MB-231	32 380 ± 5460
Breast	
SK-BR-3 ($HER2^+$)	328 281 ± 47 996
MCF-7 ($ER2^+$)	110 646 ± 17 233
Colon	
COLO 205	58 179 ± 6909
HT-29	68 ± 17
NSCLC	
Calu-3	128 201 ± 50 708
Sq. Cell Lung	
SK-MES-1	29 488 ± 5824
Acute T-Cell Leukemia	
Jurkat	0

[a]Three separate assays were performed, with the mean and standard deviation provided.

Gastrointestinal tumor xenografts stained for Trop-2 expression showed both cytoplasmic and membrane staining (Figure 1). Staining intensity correlated well with the results for surface Trop-2 expression determined by FACS analysis. For

DOI: 10.1021/acs.bioconjchem.5b00223
Bioconjugate Chem. 2015, 26, 919−931

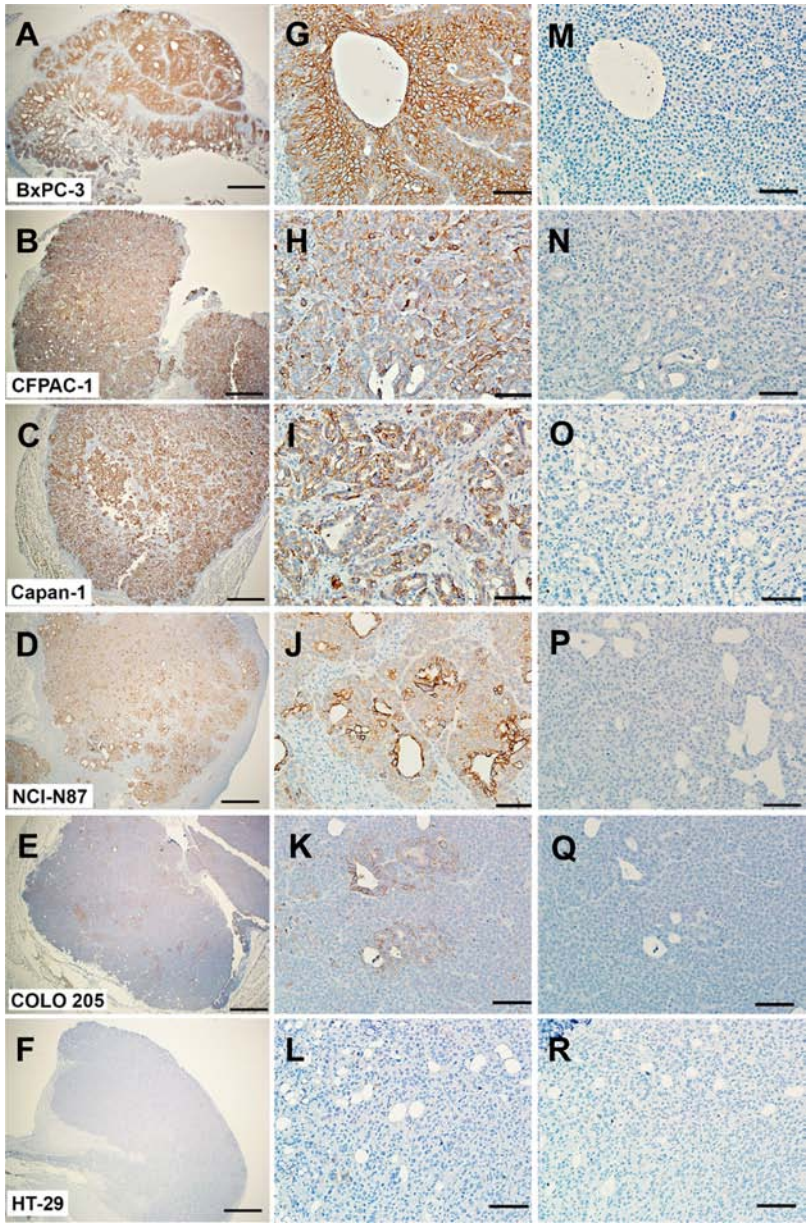

Figure 1. Trop-2 expression on various human tumor xenografts. Cells of various human carcinoma tumor lines were injected s.c. into nude mice. Once tumors appeared, they were removed and processed for IHC and stained for Trop-2 expression as described in the Experimental Procedures. (A–F) Tumors stained with goat polyclonal anti-Trop-2 antibody (bar = 1 mm). (G–L) Same tumors showing select areas of staining (bar = 100 μm). (M–R) Same area as G–L but stained with normal goat IgG (bar = 100 μm). Tumor types are pancreatic (BxPC-3, CFPAC-1, and Capan-1), gastric (NCI-N87), and colonic (COLO 205 and HT-29).

the pancreatic adenocarcinomas, all three have homogeneous staining, with BxPC-3 representing 2+ to 3+ staining. NCI-N87 gastric adenocarcinoma has a more heterogeneous staining pattern, with 3+ staining of the apical lining of the glands and less pronounced staining of surrounding tumor cells. COLO 205 demonstrates only very focal 1+ to 2+ staining, whereas HT-29 showed very rare 1+ staining of a few cells.

IMMU-132 Binding Characteristics. To further demonstrate that hRS7 does not cross-react with murine Trop-2, an ELISA was performed on plates coated with either recombinant murine Trop-2 or human Trop-2 (Figure S1). Humanized RS7 specifically bound only to the human Trop-2 (K_D = 0.3 nM); there was no cross-reactivity with the murine Trop-2. Control polyclonal rabbit anti-murine Trop-2 and anti-human Trop-2 antibodies did cross-react and bound to both forms of Trop-2 (data not shown).

IMMU-132 binding to multiple cell lines was examined, with comparison to parental hRS7 as well as to modified hRS7, hRS7-NEM (hRS7 treated with *tris*(2-carboxyethyl)phosphine (TCEP) and conjugated with *N*-ethylmaleimide) (Table S1). In all cases, calculated K_D values were in the subnanomolar range, with no significant differences among hRS7, IMMU-132, and hRS7-NEM within a given cell line.

Comparisons in binding of IMMU-132 and hRS7 were further investigated using surface plasmon resonance (BIACORE) analysis (Figure S2). A low-density Trop-2 biosensor chip (density = 1110 RU) was utilized with recombinant human Trop-2. Three independent binding runs demonstrated that IMMU-132 is not affected adversely by the SN-38-

DOI: 10.1021/acs.bioconjchem.5b00223
Bioconjugate Chem. 2015, 26, 919–931

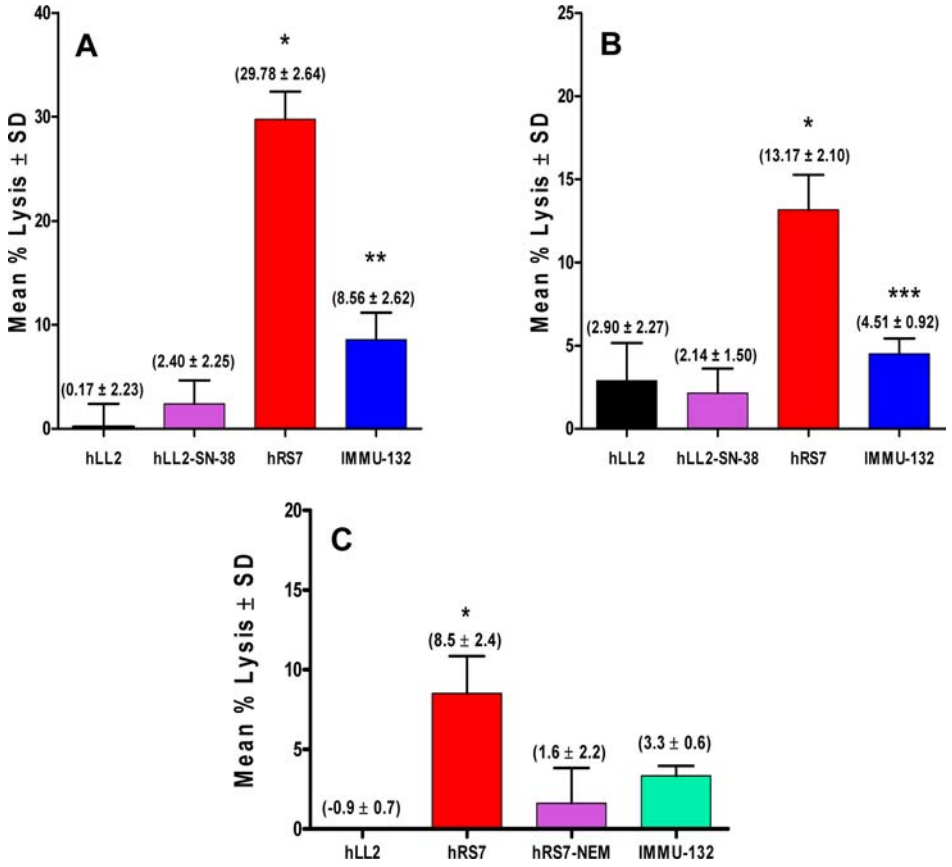

Figure 2. ADCC activity of IMMU-132. Specific cell lysis of target cells by human PBMCs mediated by IMMU-132 was compared to that with parental hRS7. Target cells were plated the night before, and the assay was performed as described in the Experimental Procedures. (A) MDA-MB-468 target cells. (B) NIH:OVCAR-3 target cells. (C) BxPC-3 target cells. *hRS7 versus all the other test agents ($P < 0.0054$). **IMMU-132 versus negative controls hLL2-SN-38 and hLL2 ($P < 0.0003$). ***IMMU-132 versus negative control hLL2-CL2A-SN-38 ($P < 0.0019$).

conjugation process as well as that it has a higher binding affinity to Trop-2 than hRS7 (0.26 ± 0.14 nM vs 0.51 ± 0.04 nM, respectively; $P = 0.0398$).

Mechanism of Action: ADCC and Intrinsic Apoptosis Signaling Pathways. Antibody-dependent cell-mediated cytotoxicity (ADCC) activity of IMMU-132 was compared to hRS7 in three different cell lines: TNBC (MDA-MB-468), ovarian (NIH:OVCAR-3), and pancreatic (BxPC-3) (Figure 2). In all three, hRS7 significantly mediated cell lysis compared to that with all other treatments, including IMMU-132 ($P < 0.0054$). ADCC decreased by more than 60% when IMMU-132 was used to target the cells as compared to that with hRS7. For example, in MDA-MB-468, specific lysis mediated by hRS7 was 29.8 ± 2.6% versus 8.6 ± 2.6% for IMMU-132 (Figure 2A; $P < 0.0001$). Similar loss in ADCC activity was likewise observed in NIH:OVCAR-3 and BxPC-3 (Figure 2, panels B and C; $P < 0.0001$ and $P < 0.0054$; respectively). This diminished ADCC activity appears to be the result of changes to the antibody during the conjugation process, since this same loss in specific cell lysis was evident with hRS7-NEM, which lacks the CL2A-SN-38 linker, having the cysteines blocked instead with *N*-ethylmaleimide (Figure 2C). There is no CDC activity associated with hRS7 or IMMU-132 (data not shown).

IMMU-132 has been shown previously to mediate the upregulation of early pro-apoptosis signaling events (p53 and $p21^{WAF1/Cip1}$), ultimately leading to the cleavage of PARP.[20] In order to better define the apoptotic pathway utilized by IMMU-132, the NCI-N87 human gastric carcinoma and BxPC-3 pancreatic adenocarcinoma cell lines were exposed to 1 μM free SN-38 or the equivalent amount of IMMU-132 (Figure 3). Both free SN-38 and IMMU-132 mediate the upregulation of $p21^{WAF1/Cip1}$, although it is not until 48 h that the upregulation between the NCI-N87 cells exposed to free SN-38 versus IMMU-132 are the same (Figure 3A), whereas in BxPC-3, maximum upregulation is evident within 24 h (Figure 3B). Both free SN-38 and IMMU-132 demonstrate cleavage of pro-caspase-9 and -7 within 48 h of exposure. Pro-caspase-3 is cleaved in both cell lines, with the highest degree of cleavage observed after 48 h. Finally, both free SN-38 and IMMU-132 mediated PARP cleavage. This first becomes evident at 24 h, with increased cleavage at 48 h. Taken together, these data confirm that the SN-38 contained in IMMU-132 has the same activity as that of free SN-38.

In addition to these later apoptosis signaling events, an earlier event associated with this pathway, namely, the phosphorylation of JNK (pJNK), is also evident in BxPC-3 cells exposed for a short time to either free SN-38 or IMMU-132 but not in those exposed to naked hRS7 (Figure 3C). Increased amounts of pJNK are evident by 4 h, with no appreciable change at 6 h. There is a higher intensity of phosphorylation in the cells exposed to free-SN-38 as compared to that with IMMU-132, but both are substantially higher than controls.

As an end point for the mechanism of action of IMMU-132, measurements of dsDNA breaks were made in BxPC-3 cells. Exposure of BxPC-3 to IMMU-132 for only 30 min resulted in

DOI: 10.1021/acs.bioconjchem.5b00223
Bioconjugate Chem. 2015, 26, 919−931

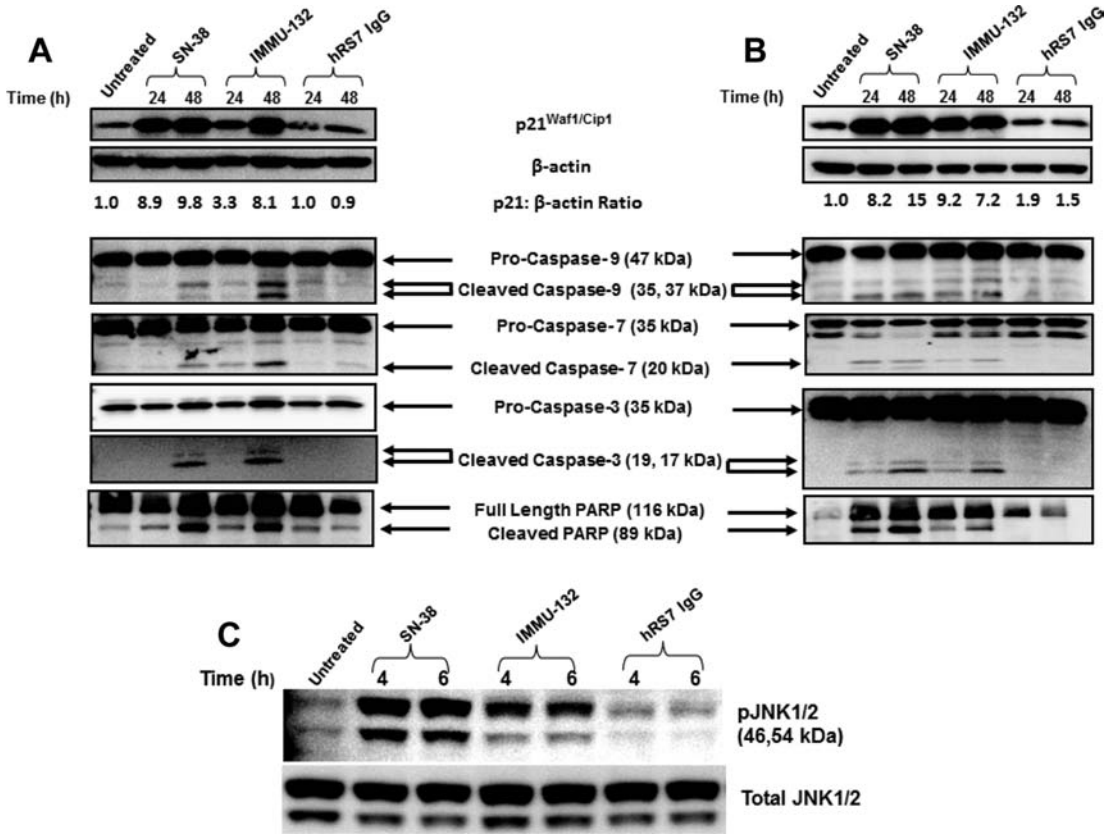

Figure 3. IMMU-132-mediated pro-apoptosis signaling in human gastric and pancreatic cancer lines. (A) NCI-N87 or (B) BxPC-3 cells were exposed to 1 μM free SN-38, the drug equivalent of IMMU-132, or protein equivalent of hRS7 for the indicated times. (C) BxPC-3 cells were exposed to the same amount of each agent described above. Cells were harvested, and western blots were performed as described in Experimental Procedures. Untreated control cells were maintained in growth medium alone until harvested after 48 h (A, B) or 6 h (C). Blots shown are representative of two separate experiments.

a greater than 2-fold induction of γH2AX when compared to that in a nontargeting control ADC (Table 2). Approximately 70% of the cells were positive for γH2AX staining versus <20% for naked hRS7, hA20-SN-38 irrelevant ADC, and untreated controls ($P < 0.0002$).

Table 2. IMMU-132-Mediated dsDNA Breaks in BxPC-3: γH2AX Induction[a]

treatment	mean fluorescence intensity	percent positive
untreated	2516 ± 191	18.8 ± 6.3
hRS7	2297 ± 18	13.0 ± 0.6
hA20-SN-38	2246 ± 58	12.7 ± 2.4
IMMU-132	5349 ± 234	69.0 ± 4.1

[a]IMMU-132 vs all three control treatments; $P < 0.0002$ (one-tailed t-test; $N = 3$).

Pharmacokinetics of IMMU-132. Binding to the human neonatal receptor (FcRn) was determined by BIACORE analysis (Figure S3). Using a low-density FcRn biosensor chip (density = 1302 RU), three independent binding runs at five different concentrations (400 to 25 nM) were conducted for each agent. Overall, both hRS7 and IMMU-132 demonstrate K_D values in the nanomolar range (92.4 ± 5.7 nM and 191.9 ± 47.6 nM, respectively), with no significant difference between the two.

Mice were injected with IMMU-132, with the clearance of IMMU-132 versus the hRS7 IgG being compared to that of parental hRS7 using two ELISAs (Figure 4). Mice injected with hRS7 demonstrated a biphasic clearance pattern (Figure 4A) that was similar to what was observed for the hRS7 targeting portion of IMMU-132 (Figure 4B), with alpha and beta half-lives of approximately 3 and 200 h, respectively. In contrast, a rapid clearance of intact IMMU-132 was observed with a half-life of 11 h and mean residence time (MRT) of 15.4 h (Figure 4C). To further confirm that disruption of interchain disulfide bonds does not alter the PK of the targeting antibody, the PK of parental hRS7 was compared to that of modified hRS7 (hRS7-NEM). There were no significant differences noted between either agent in terms of half-life, C_{max}, AUC, clearance, or MRT (Figure S4).

IMMU-132 Efficacy in Human Gastric Carcinoma Xenografts. Efficacy of IMMU-132 has been demonstrated previously in non-small-cell lung, colon, TNBC, and pancreatic carcinoma xenograft models.[20,23] To further extend these findings to other gastrointestinal cancers, IMMU-132 was tested in mice bearing a human gastric carcinoma xenograft, NCI-N87 (Figure 5). Treatment with IMMU-132 achieved significant tumor regressions compared to that with saline and nontargeting hA20 (anti-CD20)−SN-38 ADC controls (Figure 5A; $P < 0.001$). There were 6 of 7 mice in the IMMU-132 group that were partial responders that lasted for more than 18 days after the last therapy dose was administered to the animals. This resulted in a mean time to progression (TTP) of 41.7 ± 4.2 days compared to no responders in the control ADC group, with a TTP of 4.1 ± 2.0 days ($P < 0.0001$). Overall, the median

DOI: 10.1021/acs.bioconjchem.5b00223
Bioconjugate Chem. 2015, 26, 919−931

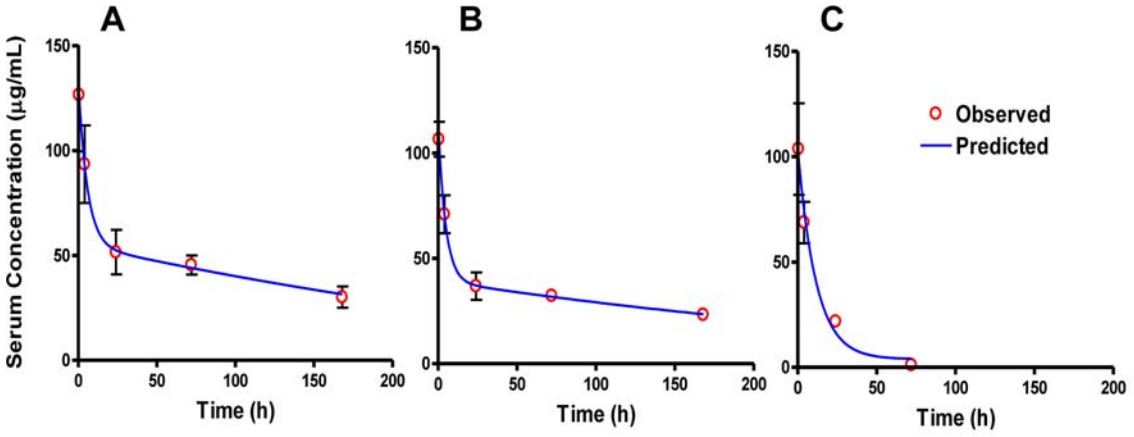

Pharmacokinetic parameters estimated from the above referenced clearance curves

Drug	$T_{½\alpha}$ (h)	$T_{½\beta}$ (h)	AUC (h*μg/mL)	CL (mL/h)	C_{Max} (μg/mL)	MRT (h)
Unconjugated hRS7	3.9	195	16239	0.012	133.3	273.6
hRS7 Moiety of IMMU-132	3.2	224	13112	0.015	115.0	314.2
IMMU-132 (intact)	11	N.A.	1516	0.133	103.6	15.4

N.A., not applicable

Figure 4. Pharmacokinetics of IMMU-132 in mice. Naïve nude mice (N = 5) were injected i.v. with 200 μg of IMMU-132. At various time points, these mice were bled, and serum was obtained and analyzed for intact conjugate and carrier hRS7 antibody, as described in the Experimental Procedures. For comparison, another group of mice was injected with 200 μg of parental hRS7. (A) Serum concentration and clearance of hRS7 from parental control injected mice. Concentration and clearance of (B) hRS7 carrier antibody versus (C) intact conjugate from IMMU-132-injected mice. Graphed data shown as mean ± SD. N.A., not applicable.

survival time (MST) for IMMU-132-treated mice was 66 days versus 24 days for control ADC and 14 days for saline control animals (Figure 5B; P < 0.0001).

Clinically-Relevant Dosing Schemes. The highest repeated doses tolerated of IMMU-132 currently being tested clinically are 8 and 10 mg/kg given on days 1 and 8 of 21 day cycles.[23,24] A human dose of 8 mg/kg translates to a murine dose of 98.4 mg/kg, or approximately 2 mg to a 20 g mouse. Three different dose schedules of fractionated 2 mg of IMMU-132 were examined in a human pancreatic adenocarcinoma xenograft model (BxPC-3). This total dose was fractionated using one of three different dosing schedules: one group received two IMMU-132 doses of 1 mg (therapy days 1 and 15), one received four doses of 0.5 mg (therapy days 1, 8, 22, and 29), and the final group eight doses of 0.25 mg (therapy days 1, 4, 8, 11, 22, 25, 29, and 32). All three dosing schemes provided a significant antitumor effect when compared to that in untreated control animals, both in terms of tumor growth inhibition and overall survival (Figure 6A; P < 0.0009 and P < 0.0001, respectively). There are no significant differences in TTP between the three different treatment groups, which ranged from 22.4 ± 10.1 days for the 1 mg dosing group to 31.7 ± 14.5 days for the 0.25 mg dosing group (TTP for untreated control group = 5.0 ± 2.3 days).

A similar dose schedule experiment was performed in mice bearing NCI-N87 human gastric tumor xenografts (Figure 6B). All three dose schedules had a significant antitumor effect when compared to that of untreated control mice but were not different from each other (AUC; P < 0.0001). Likewise, in terms of overall survival, while all three dose schedules provided a significant survival benefit when compared to that of the untreated control (P < 0.0001), there were no differences among any of these three different schedules.

To further discriminate possible dosing schemes, mice bearing NCI-N87 tumors were subjected to chronic IMMU-132 dosing in which mice received 0.5 mg injections of IMMU-132 once a week for 2 weeks followed by 1 week off before starting another cycle (Figure 6C), as in the current clinical trial schedule. In all, four treatment cycles were administered to the animals. This dosing schedule slowed tumor growth with a TTP of 15.7 ± 11.1 days versus 4.7 ± 2.2 days for control ADC-treated mice (P = 0.0122). Overall, chronic dosing increased the median survival 3-fold from 21 days for control ADC-treated mice to 63 days for those animals administered IMMU-132 (P = 0.0001). Importantly, in all of these different dosing scheme evaluations, no treatment-related toxicities were observed in the mice, as demonstrated by no significant loss in body weight (data not shown).

DISCUSSION

In a current Phase I/II clinical trial (ClinicalTrials.gov, NCT01631552), IMMU-132 (sacituzumab govitecan) is demonstrating objective responses in patients presenting with a wide-range of solid tumors.[31,32] As this Phase I/II clinical trial continues, efficacy of IMMU-132 needs to be further explored in an expanding list of Trop-2-positive cancers. Additionally, the uniqueness of IMMU-132, in contrast to other clinically relevant ADCs that make use of ultratoxic drugs, needs to be

DOI: 10.1021/acs.bioconjchem.5b00223
Bioconjugate Chem. 2015, 26, 919−931

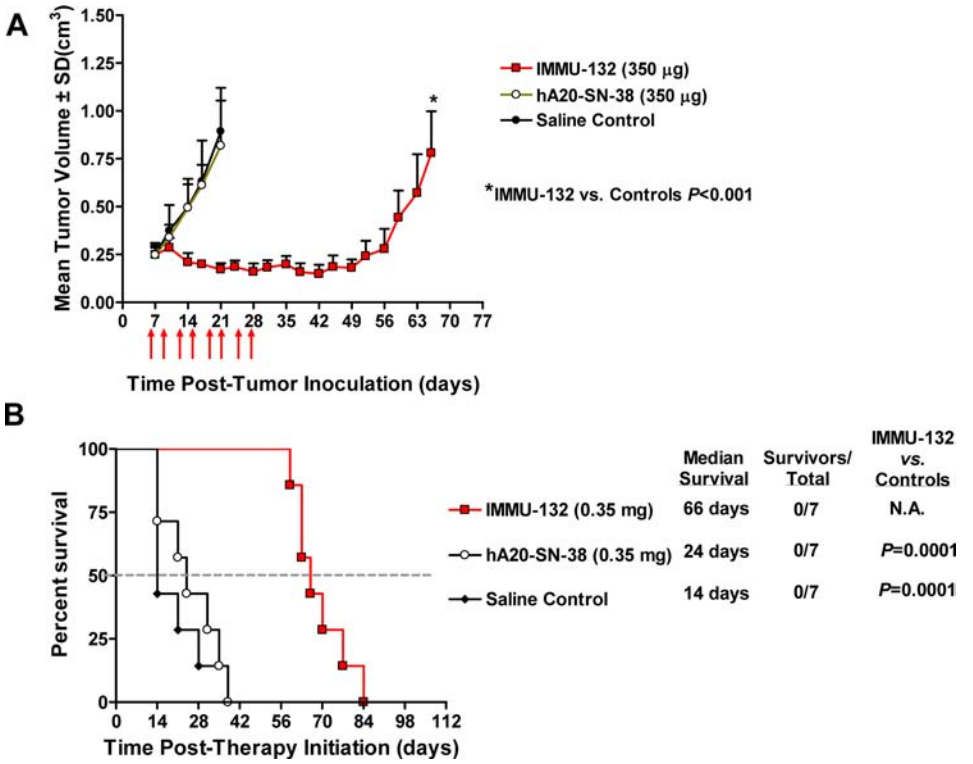

Figure 5. Efficacy of IMMU-132 in mice bearing human gastric carcinoma xenograft. Mice bearing NCI-N87 human gastric tumors (TV = 0.249 ± 0.049 cm^3) were treated with 0.35 mg of IMMU-132 twice weekly for 4 weeks. (A) Mean tumor growth curves for IMMU-132 treated animals compared to those for saline and non-tumor-targeting control ADC, hA20-CL2A-SN-38, treated mice. Arrows indicate therapy days. (B) Survival curves for treated mice with a disease end point of tumor progression greater than 1.0 cm^3.

further elucidated as we move forward in its clinical development. The work presented here further characterizes IMMU-132 and demonstrates its efficacy against gastric and pancreatic adenocarcinomas at clinically relevant dosing schemes.

The prevailing view of a successful ADC is that it should use an antibody recognizing an antigen with high tumor expression levels relative to that in normal tissue and one that preferably internalizes when bound to the tumor cells.[17] All of the currently approved ADCs have used an ultratoxic drug (picomolar IC_{50}) coupled to the antibody by a highly stable linker at low substitution ratios (2−4 drugs per antibody). IMMU-132 diverges from this paradigm in three main aspects: (i) SN-38, a moderately cytotoxic drug (nanomolar IC_{50}), is used as the chemotherapeutic agent, (ii) SN-38 is conjugated site-specifically to 8 interchain thiols of the antibody, yielding a substitution of 7.6 drugs per antibody, and (iii) a carbonate linker is used that is cleavable at low pH but will also release the drug with a half-life in serum of ∼24 h.[20] IMMU-132 is composed of an antibody that internalizes after binding to an epitope, as we have shown, that is specific for human Trop-2, which is highly expressed on many different types of epithelial tumors as well as at lower concentrations in their corresponding normal tissues.[21] Despite the presence in normal tissues, prior studies in monkeys, which also express Trop-2 in similar tissues, indicated relatively mild and reversible histopathological changes even at very high doses where dose-limiting neutropenia and diarrhea occurred, suggesting that the antigen in the normal tissues was sequestered in some manner or that the use of a less toxic drug spared these normal tissues from severe damage.[20]

Herein, we expanded an assessment of Trop-2 expression on multiple human solid tumor lines, examining *in vitro* expression in a more quantitative manner than reported previously[20] but also, importantly, in xenografts that illustrate Trop-2 expression ranging from homogeneous (e.g., NCI-N87) to very focal (e.g., COLO 205). Overall, surface expression levels of Trop-2 determined *in vitro* correlated with staining intensity upon IHC analysis of xenografts. It is particularly interesting that even in a tumor like COLO 205, where there are only focal pockets of Trop-2-expressing cells revealed by immunohistology, IMMU-132 was still capable of eliciting specific tumor regressions, suggesting that a bystander effect may occur as a result of the release of SN-38 from the conjugate bound to the antigen-presenting cells.[20] Indeed, SN-38 readily penetrates cell membranes and therefore its local release within the tumor microenvironment provides another mechanism for its entry into cells without requiring internalization of the intact conjugate. Importantly, the SN-38 bound to the conjugate remains in a fully active state, in other words, it is not glucuronidated and would be in the lactone ring form at the time of release.[33] This property is unique, distinguishing IMMU-132's ability to localize a fully active form of SN-38 in a more selective manner than any of the other slow-release SN-38 or irinotecan agents studied to date.

The Phase I clinical trial with IMMU-132 identified 8−10 mg/kg given weekly for 2 weeks on a 21 day cycle for further investigation in Phase II.[32] Patients with a wide range of metastatic solid tumors, including pancreatic and gastric cancers, have shown extended periods of disease stabilization after relapsing to multiple prior therapies.[23,24,32,34,35] Additional studies in xenograft models were undertaken to determine if different dosing schedules may be more efficacious. To this end,

DOI: 10.1021/acs.bioconjchem.5b00223
Bioconjugate Chem. 2015, 26, 919−931

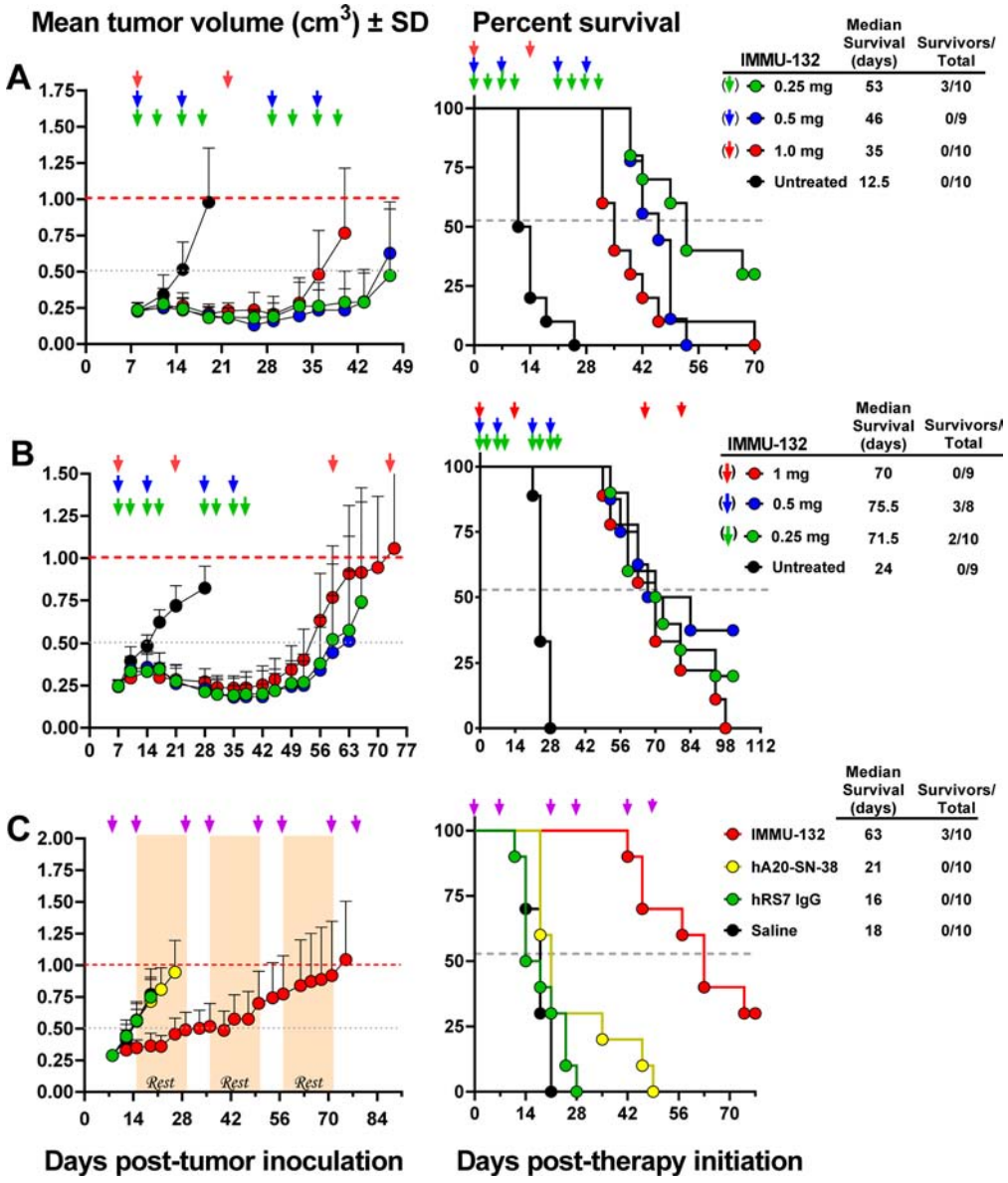

Figure 6. Various IMMU-132 dosing schemes in mice bearing pancreatic and gastric tumor xenografts. Nude mice (N = 8−10) bearing s.c. BxPC-3 or NCI-N87 xenografts were as described in Experimental Procedures. (A) BxPC-3-bearing mice were treated (arrows) with two cycles of IMMU-132 at 1 mg every 14 days, 0.5 mg weekly for 2 weeks, or 0.25 mg twice weekly for 2 weeks, totaling 2 mg IMMU-132 to all the mice. (B) Similar dosing of NCI-N87-bearing mice (arrows), with mice in the 1 mg treatment group receiving one additional cycle. (C) Chronic dosing of IMMU-132 in mice bearing NCI-N87, using 0.5 mg once weekly for 2 weeks in a 3 week treatment cycle for a total of 4 cycles. Corresponding survival curves (end point: tumor progression > 1.0 cm^3) are shown to right of each tumor growth curve.

the equivalent to the human dose of 8 mg/kg (mouse dose of 98.4 mg/kg) was fractionated over three different dosing schedules, including every other week, weekly, or twice-weekly on a 21 day cycle. In the pancreatic and gastric tumor models, no significant difference in therapeutic responses were observed for all three schedules, with tumors progressing only after therapy was discontinued. Therefore, these data support the continued use of the once-weekly dosing regimen currently being pursued clinically.

With clinical trials recommending an IMMU-132 each treatment dose of 8−10 mg/kg,[32] it was important to examine whether the antibody alone might contribute to the IMMU-132's activity. Previous studies in nude mice−human xenograft models had included unconjugated hRS7 IgG alone (e.g., repeated doses of 25 to 50 mg/kg), with no evidence of therapeutic activity;[20] however, studies in mice cannot always predict immunological functionality. ADCC activity of hRS7 *in vitro* has been reported in Trop-2-positive ovarian and uterine carcinomas.[36−40] We confirmed unconjugated hRS7 ADCC activity in three different cells lines, but we found that IMMU-132 lost 60−70% of its effector function. Since the reduced/NEM-blocked IgG has a similar loss of ADCC activity, it appears that the attachment of the CL2A-SN-38 component was not, in itself, responsible.

Antibodies also can elicit cell death by acting on various apoptotic signaling pathways. However, we did not observe any effects of the unconjugated antibody in a number of apoptotic signaling pathways,[25−29] but, instead, we noted that IMMU-132 elicited similar intrinsic apoptotic events as those from SN-38.[30] Early events include the phosphorylation of JNK1/2 as well as

DOI: 10.1021/acs.bioconjchem.5b00223
Bioconjugate Chem. 2015, 26, 919−931

the upregulation of $p21^{WAF1/Cip1}$, leading to the activation of caspase-9, -7, and -3, with the end result being PARP cleavage and significant levels of dsDNA breaks, as measured by increased amounts of phosphorylated histone H2AX (γH2AX).[41] These data suggest that IMMU-132's primary mechanism of action is related to SN-38.

Surface plasmon resonance (BIACORE) analysis did not detect a significant difference in IMMU-132's binding to the human neonatal receptor (FcRn), despite the average binding levels being ~2-fold lower for IMMU-132. FcRn binding has been linked to an extended IgG half-life in serum,[42] but because an antibody's affinity for FcRn *in vitro* may not correlate with *in vivo* clearance rates,[43] the overall importance of this finding is unknown. Previous experiments in tumor-bearing mice using ^{111}In-DTPA-IMMU-132 revealed that the conjugate cleared at a somewhat faster rate from the serum than ^{111}In-DTPA-hRS7, although both had similar tumor uptake.[20] In the current studies, an ELISA assay that also measured the clearance of the IgG component found IMMU-132 and the reduced and NEM-blocked IgG cleared at similar rates as those of unconjugated hRS7, suggesting that the coupling to the interchain disulfides does not destabilize the antibody. As expected, when using an ELISA that monitored the clearance of the intact conjugate (capturing using an anti-SN-38 antibody and probe with an anti-idiotype antibody), its clearance rate was faster than that when monitoring only the IgG component. This difference simply reflects SN-38's release from the conjugate with a half-life of ~1 day. We also have examined the clearance rates of hRS7-SN-38 conjugates prepared at different substitution levels by ELISA and again found no appreciable difference in their clearance rates.[44] Overall, these data suggest that mild reduction of the antibody, with the subsequent site-specific modification of some or all interchain disulfides, has minimal if any impact on the serum clearance of the IgG, but IMMU-132's overall clearance rate will be defined largely by the rate of SN-38 from the linker.

Additionally, extensive cell-binding experiments demonstrated no significant difference in the binding of IMMU-132, the unconjugated antibody, or the NEM-modified antibody, suggesting that the site-specific linkage to the interchain disulfides protects the antigen-binding properties of the antibody. Interestingly, when analyzed by BIACORE, which more accurately measures the on and off rates in addition to overall affinity, IMMU-132 had a significant 2-fold improvement in calculated K_D values for Trop-2 binding when compared to those of naked hRS7. We speculate that this improvement may be result of the added hydrophobicity when SN-38 is conjugated to the antibody. Hydrophobic residues, as well as hydrophobicity of enclosed regions of protein binding sites, have been shown to impart a stronger affinity for the epitope.[45−47] These regions do not have to be at the protein−protein interface but can lie in surrounding, less energetic contact residues.[48] While none of the SN-38 conjugation sites are present in the complement-determining regions (CDR) of hRS7, the prospects that the SN-38 on the antibody may displace some of the water molecules around the epitope, resulting in the improved binding affinity observed for IMMU-132 relative to that of naked hRS7, cannot be discounted.

Most efforts in ADC development have been directed toward using a stable linker and an ultratoxic drug, with preclinical studies indicating the specific optimal requirements for those conjugates.[17,49] For example, a comparison of T-DM1 to another less stable derivative, T-SSP-DM1, revealed that intact T-SSP-DM1 cleared at an approximately 2-fold faster rate than T-DM-1 in non-tumor-bearing mice,[49,50] with 1.5-fold higher levels of T-DM1 compared to T-SSP-DM1 in the tumors. Unexpectedly, and most interesting, was the finding that the amount of free, active maytansinoid catabolites in the targeted tumors was very similar between the two ADCs.[50] In other words, T-SSP-DM1 was able to overcome its deficiencies in linker stability due to the fact that the lower stability resulted in more efficient release of the drug at the tumor than the more stable T-DM1. Not surprisingly, this equivalency of active drug catabolite between the two ADCs in the tumors resulted in similar antitumor effects in tumor-bearing animals. Ultimately, T-DM1 was chosen based on toxicity issues that arise when using an ultratoxic drug and less stable linkers.[49] Since SN-38 is at least a log-fold less toxic than these maytansines, its release from the ADC is expected to have less toxicity. However, even with its release in serum, the amount of SN-38 localized in human gastric or pancreatic tumor xenografts was up to 136-fold higher than in tumor-bearing mice injected with irinotecan doses that had a >20-fold higher SN-38 equivalent.[23,33] While we have tested more stable linkers in the development of IMMU-132, they were significantly less effective in xenograft tumor models than IMMU-132.[51] Similarly, linkers that released SN-38 more quickly (e.g., serum half-life of ~10 h) also were less effective in xenograft models,[52,53] suggesting that there is an optimal window within which the release of SN-38 leads to improved efficacy. Thus, current data demonstrate that IMMU-132 is a more efficient way to target and release the drug at the tumor than irinotecan. Early clinical studies have shown encouraging objective responses in various solid tumors and importantly have indicated a better safety profile, with a lower incidence of diarrhea, than irinotecan therapy.[23,24,31,32,34,35]

In summary, IMMU-132 (sacituzumab govitecan) is a paradigm shift in ADC development. It uses a moderately stable linker to conjugate 7 to 8 molecules of the more tolerable active metabolite of irinotecan, SN-38, to an anti-Trop-2 antibody. Despite these seemingly counterintuitive characteristics vis-à-vis ultratoxic ADCs, nonclinical studies have demonstrated that IMMU-132 very effectively targets Trop-2-expressing tumors with significant efficacy and no appreciable toxicity. In early Phase I/II clinical trials against a wide range of solid tumors, including pancreatic, gastric, TNBC, and small-cell and non-small-cell lung carcinomas, IMMU-132 is likewise exhibiting antitumor effects with manageable toxicities in these patients, with no immune responses to either the IgG or SN-38 detected, even after many months of dosing.[23,24,31,32,34,35] Given the elevated expression of Trop-2 on such a wide variety of solid tumors, IMMU-132 continues to be studied clinically, especially in advanced cancers that have been refractory to most current therapy strategies.

EXPERIMENTAL PROCEDURES

Cell Lines and Chemotherapeutics. All human cancer cell lines used were purchased from the American Type Culture Collection (ATCC) (Manassas, VA). Each was maintained according to the recommendations of ATCC and routinely tested for mycoplasma using MycoAlert mycoplasma detection kit (Lonza, Rockland, ME) and all were authenticated by short tandem repeat (STR) assay by the ATCC. IMMU-132 (hRS7-SN-38) and control ADCs (anti-CD20 hA20-SN-38 and anti-CD22 hLL2-SN-38) were made as previously described and stored at −20 °C.[20] SN-38 was purchased (Biddle Sawyer

DOI: 10.1021/acs.bioconjchem.5b00223
Bioconjugate Chem. 2015, 26, 919−931

Pharma, LLC, New York, NY) and stored in 1 mM aliquots in DMSO at −20 °C.

Trop-2 ELISA. Recombinant human Trop-2 with a His-tag (Sino Biological, Inc., Bejing, China; cat. no. 10428-H09H) and recombinant mouse Trop-2 with a His-Tag (Sino Biological, Inc., cat. no. 50922-M08H) were plated onto Ni-NTA Hissorb strips (Qiagen GmbH cat. no. 35023) at 1 μg for 1 h at room temperature. The plate was washed four times with PBS−Tween (0.05%) wash buffer. Serial dilutions of hRS7 were made in 1% BSA−PBS dilution buffer to a test range of 0.1 ng/mL to 10 μg/mL. The plates were then incubated for 2 h at room temperature before being washed four times followed by the addition of a peroxidase-conjugated secondary antibody (affinipure goat anti-human, Fc fragment specific; Jackson Immunoresearch cat. no. 109-036-098). After a 45 min incubation, the plate was washed, and a substrate solution (*o*-phenylenediamine dihydrochloride (OPD); Sigma, cat. no. P828) was added to all the wells. Plates were incubated in the dark for 15 min before the reaction was stopped with 4 N sulfuric acid. The plates were read at 450 nm on Biotek ELX808 plate reader. Data were analyzed and graphed using Prism GraphPad software (v4.03) (Advanced Graphics Software, Inc.; Encinitas, CA).

***In Vitro* Cell Binding.** LumiGLO chemiluminescent substrate system (KPL, Gaithersberg, MD) was used to detect antibody binding to cells. Briefly, cells were plated into a 96 black-well, flat, clear-bottom plate overnight. Antibodies were serially diluted 1:2 and added in triplicate, yielding a concentration range from 0.03 to 66.7 nM. After incubating for 1 h at 4 °C, the media was removed, and the cells were washed with fresh cold media followed by the addition of a 1:20000 dilution of goat-anti-human horseradish peroxidase-conjugated secondary antibody (Jackson Immunoresearch, West Grove, PA) for 1 h at 4 °C. The plates were again washed before the addition of the LumiGLO reagent. Plates were read for luminescence using an Envision plate reader (PerkinElmer, Boston MA). Data were analyzed by nonlinear regression to determine the equilibrium dissociation constant (K_D). Statistical comparisons of K_D values were made with Prism GraphPad software (v4.03) (Advanced Graphics Software, Inc.; Encinitas, CA) using an F-test on the best-fit curves for the data. Significance was set at $P < 0.05$.

Antibody-Dependent Cell-Mediated Cytotoxicity (ADCC). A 4 h LDH-release assay was performed to evaluate ADCC activity elicited by IMMU-132, hRS7 IgG, hLL2-SN-38, and hLL2 IgG (hLL2 are nonbinding anti-CD22 conjugates for the solid tumor cell lines). Briefly, target cells (MDA-MB-468, NIH:OVCAR-3, or BxPC-3) were plated at 1×10^4 cells/well in a 96-well, black, flat-bottom plate and incubated overnight. The next day, peripheral blood mononuclear effector cells (PBMCs) were freshly isolated from a donor and added to assigned wells on the reaction plate at an E:T ratio of 50:1. Acquisition of human PBMCs was done under the approval of the New England Institutional Review Board (Newton, MA). Test reagents were added to their assigned wells at a final concentration of 33.3 nM. One set of wells received ADCC assay medium alone for background control, and another set of wells received cells alone plus Triton X-100 for maximum cell lysis control. The plate was incubated for 4 h at 37 °C. After 4 h, target cell lysis was assessed by a homogeneous fluorometric LDH release assay (Cyto Tox-One homogenous membrane integrity assay; Promega, cat. no. G7891). The plates were read (544−590 nm) using an Envision plate reader (PerkinElmer LAS, Inc.; Shelton, CT). Data were analyzed by Microsoft Excel. Percent specific lysis was calculated as follows

$$\%\ \text{specific lysis} = \frac{\text{experimental} - (\text{effector} + \text{target control})}{\text{max . lysis} - (\text{target control})} \times 100$$

where

experimental: effector + target cells + antibody

effector + target control: effector + target cells

max . lysis: target cells + Triton X-100

target control: target cells only

Surface Plasmon Resonance Binding (BIACORE). Briefly, rhTrop-2/TACSTD2 (Sino Biological, Inc.) or recombinant human neonatal receptor (FcRn), produced as described,[54] was immobilized with an amine coupling kit (GE Healthcare; cat. no. BR-1000−50) on a CM5 sensor chip (GE Healthcare; cat. no. BR-1000−12) following the manufacture's instructions for a low-density chip. Three separate sets of dilutions of hRS7 IgG and IMMU-132 were made in running buffer (400, 200, 100, 50, and 25 nM). Each set would make up a separate run on the BIACORE (BIACORE-X; Biacore Inc., Piscataway, NJ), and data were analyzed using BIAevaluation software (Biacore Inc., v4.1). Analysis was performed with a 1:1 (Langmuir) binding model and fit using all five concentration points for each sample run to determine the best fit (lowest χ^2 value). The K_D value was calculated using the formula $K_D = k_d1/k_a1$, where k_d1 is the dissociation rate constant and k_a1 is the association rate constant.

Immunohistological Assessment of the Distribution of Trop-2 in Formalin-Fixed, Paraffin-Embedded Tissues. Tumor xenografts were taken from mice, fixed in 10% buffered formalin, and paraffin-embedded. After deparaffination, 5 μm sections were incubated with Tris/EDTA buffer (DaKo target retrieval solution, pH 9.0; Dako, Denmark) at 95 °C for 30 min in a NxGen decloaking chamber (Biocare Medical, Concord, CA). Trop-2 was detected with a goat polyclonal anti-human Trop-2 antibody at 10 μg/mL (R&D Systems, Minneapolis, MN) and stained with Vector Vectastain ABC kit (Vector Laboratories, Inc., Burlingame, CA). Normal goat antibody was used as the negative control (R&D Systems, Minneapolis, MN). Tissues were counterstained with hematoxylin for 6 s.

Trop-2 Surface Expression on Human Carcinoma Cell Lines. Expression of Trop-2 on the cell surface is based on flow cytometry. Briefly, cells were harvested with Accutase cell detachment solution (Becton Dickinson (BD), Franklin Lakes, NJ; cat. no. 561527) and assayed for Trop-2 expression using QuantiBRITE PE beads (BD cat. no. 340495) and a PE-conjugated anti-Trop-2 antibody (eBiosciences, cat. no. 12-6024) following the manufacture's instructions. Data were acquired on a FACSCalibur flow cytometer (BD) with CellQuest Pro software. Staining was analyzed with Flowjo software (Tree Star, Ashland, OR).

Pharmacokinetics. All animal studies were approved by Rutgers School of Biomedical and Health Sciences Institutional Animal Care and Use Committee. Naïve female NCr nude (*nu/nu*) mice, 8−10 weeks old, were purchased from Taconic Farms (Germantown, NY). Mice ($N = 5$) were injected i.v. with 200 μg of IMMU-132, parental hRS7, or modified hRS7-NEM

DOI: 10.1021/acs.bioconjchem.5b00223
Bioconjugate Chem. 2015, 26, 919−931

(hRS7 treated with TCEP and conjugated with *N*-ethylmaleimide). Animals were bled via retroorbital plexis at 30 min and 4, 24, 72, and 168 h postinjection. ELISA was utilized to determine serum concentrations of total hRS7 IgG by competing for the binding to an anti-hRS7 IgG idiotype antibody with a horseradish peroxidase conjugate of hRS7. Serum concentrations of intact IMMU-132 were determined using an anti-SN-38 antibody to capture and a horseradish peroxidase-conjugated anti-hRS7 IgG antibody to detect. Pharmacokinetic (PK) parameters were computed by noncompartmental analysis using Phoenix WinNonlin software (version 6.3; Pharsight Corp., Mountainview, CA).

Assessment of Double-Stranded DNA Breaks *In Vitro*. For drug activity testing, BxPC-3 cells were seeded in 6-well plates at 5×10^5 cells/well and held at 37 °C overnight. After 10 min cooling on ice, cells were incubated with IMMU-132, hA20-SN-38, or hRS7-IgG at a final concentration of 20 μg/mL for 30 min on ice, washed three times with fresh media, and then returned to 37 °C to continue culture overnight. The following morning, cells were trypsinized briefly, spun down, stained with Fixable viability stain 450 (BD Biosciences, San Jose, CA), washed with 1% BSA−PBS, fixed in 4% formalin for 15 min, washed again, and permeabilized in 0.15% Triton X-100 in PBS for another 15 min. After washing twice with 1% BSA−PBS, cells were incubated with mouse anti-γH2AX-AF488 (EMD Millipore Corporation, Temecula, CA) for 45 min at 4 °C. The signal intensity of γH2AX was measured by flow cytometry using a BD FACSCanto (BD Biosciences, San Jose, CA).

***In Vivo* Therapeutic Studies.** NCr female athymic nude (*nu*/*nu*) mice, 4−8 weeks old, were purchased from Taconic Farms (Germantown, NY). NCI-N87 gastric tumor xenografts were established by harvesting cells from tissue culture and making a final cell suspension 1:1 in Matrigel (BD Bioscience, San Jose, CA), with each mouse receiving a total of 1×10^7 cells s.c. in the right flank. For BxPC-3, xenografts of 1 g were harvested, and a tumor suspension was made in HBSS to a concentration of 40% tumor w/v. This suspension was mixed 1:1 with Matrigel for a final tumor suspension of 20% w/v. Mice were then injected with 300 μL s.c. Tumor volume (TV) was determined by measurements in two dimensions using calipers, with volume defined as $L \times w^2/2$, where L is the longest dimension of the tumor and w, the shortest. For IHC, tumors were allowed to grow to approximately 0.5 cm^3 before the mice were euthanized and the tumors were removed, formalin-fixed, and paraffin-embedded. For therapy studies, mice were randomized into treatment groups, and therapy began when tumor volumes were approximately 0.25 cm^3. Treatment regimens, dosages, and number of animals in each experiment are described in the Results and in the figure captions. The lyophilized IMMU-132 and control ADC (hA20-SN-38) were reconstituted and diluted as required in sterile saline.

Mice were euthanized and deemed to have succumbed to disease once tumors grew to greater than 1.0 cm^3 in size. Best responses to therapy were defined as partial response, shrinking >30% from starting size; stable disease, tumor volumes shrinking up to 29% or increase no greater than 20% of initial size; progression, tumors increase ≥20% either from their starting size or from their nadir. Time to progression (TTP) was determined as time post-therapy initiation when the tumor grew more than 20% in size from its nadir.

Statistical analysis of tumor growth was based on area under the curve (AUC). Profiles of individual tumor growth were obtained through linear-curve modeling. An F-test was employed to determine equality of variance between groups prior to statistical analysis of growth curves. A two-tailed *t*-test was used to assess statistical significance between the various treatment groups and controls, except for the saline control, where a one-tailed *t*-test was used (significance at $P \leq 0.05$). Survival studies were analyzed using Kaplan−Meier plots (log-rank analysis), using Prism GraphPad software (v4.03) (Advanced Graphics Software, Inc., Encinitas, CA).

Immunoblotting. Cells (2×10^6) were plated in 6-well plates overnight. The following day, they were treated with either free SN-38 (dissolved in DMSO) or IMMU-132 at an SN-38 concentration equivalent to 0.4 μg/mL (1 μM). Parental hRS7 was used as a control for the ADC. Cells were lysed in buffer containing 10 mM Tris, pH 7.4, 150 mM NaCl, protease inhibitors, and phosphatase inhibitors (2 mM Na_2PO_4, 10 mM NaF). A total of 20 μg of protein was resolved in a 4−20% SDS polyacrylamide gel, transferred onto a nitrocellulose membrane, and blocked by 5% nonfat milk in 1× TBS-T (Tris-buffered saline, 0.1% Tween-20) for 1 h at room temperature. Membranes were probed overnight at 4 °C with primary antibodies followed by 1 h incubation with anti-rabbit secondary antibody (1:2500) at room temperature. Signal detection was done using a chemiluminescence kit (Supersignal West Dura, Thermo Scientific, Rockford, IL) with the membranes visualized on a Kodak Image Station 40000R. Primary antibodies $p21^{Waf1/Cip1}$ (cat. no. 2947), caspase-3 (cat. no. 9665), caspase-7 (cat. no. 9492), caspase-9 (cat. no. 9502), PARP (cat. no. 9542), β-actin (cat. no. 4967), pJNK1/2 (cat. no. 4668), JNK (cat. no. 9258), and goat anti-rabbit-HRP secondary antibody (cat. no. 7074) were obtained from Cell Signal Technology (Danvers, MA).

■ ASSOCIATED CONTENT

Supporting Information

Table S1: Cell binding/avidity of IMMU-132, hRS7, and hRS7-NEM on various Trop-2-positive solid tumor lines. Figure S1: Specificity of hRS7 for human Trop-2. Figure S2: IMMU-132 vs hRS7 binding to Trop-2 via BIACORE. Figure S3: IMMU-132 vs hRS7 binding to human neonatal receptor via BIACORE. Figure S4: Comparison of PK between hRS7 and hRS7-NEM in mice. The Supporting Information is available free of charge on the ACS Publications website at DOI: 10.1021/acs.bioconjchem.5b00223.

■ AUTHOR INFORMATION

Corresponding Authors

*(T.M.C.) Telephone: 973-605-8200 ext. 179; Fax: 973-605-1340; E-mail: tcardillo@immunomedics.com.

*(D.M.G.) Telephone: 973-605-8200 ext. 7128; Fax: 973-605-8282; E-mail: dmg.gscancer@att.net.

Notes

The authors declare the following competing financial interest(s): All the authors have employment and other financial relationships with Immunomedics, Inc.

■ ACKNOWLEDGMENTS

We thank Nalini Sathyanarayan and Christine Mazza-Ferreira for contributions to synthetic and conjugation chemistries and

DOI: 10.1021/acs.bioconjchem.5b00223
Bioconjugate Chem. 2015, 26, 919−931

Maria Zalath and Gaby Terracina for their assistance with the animal studies.

REFERENCES

(1) Siegel, R., Ma, J., Zou, Z., and Jemal, A. (2014) Cancer statistics, 2014. *CA−Cancer J. Clin. 64*, 9−29.
(2) Cubas, R., Li, M., Chen, C., and Yao, Q. (2009) Trop2: a possible therapeutic target for late stage epithelial carcinomas. *Biochim. Biophys. Acta 1796*, 309−314.
(3) Ambrogi, F., Fornili, M., Boracchi, P., Trerotola, M., Relli, V., Simeone, P., La Sorda, R., Lattanzio, R., Querzoli, P., Pedriali, M., et al. (2014) Trop-2 is a determinant of breast cancer survival. *PLoS One 9*, e96993.
(4) Liu, T., Liu, Y., Bao, X., Tian, J., Liu, Y., and Yang, X. (2013) Overexpression of TROP2 predicts poor prognosis of patients with cervical cancer and promotes the proliferation and invasion of cervical cancer cells by regulating ERK signaling pathway. *PLoS One 8*, e75864.
(5) Fang, Y. J., Lu, Z. H., Wang, G. Q., Pan, Z. Z., Zhou, Z. W., Yun, J. P., Zhang, M. F., and Wan, D. S. (2009) Elevated expressions of MMP7, TROP2, and survivin are associated with survival, disease recurrence, and liver metastasis of colon cancer. *Int. J. Colorectal Dis. 24*, 875−884.
(6) Nakashima, K., Shimada, H., Ochiai, T., Kuboshima, M., Kuroiwa, N., Okazumi, S., Matsubara, H., Nomura, F., Takiguchi, M., and Hiwasa, T. (2004) Serological identification of Trop-2 by recombinant cDNA expression cloning using sera of patients with esophageal squamous cell carcimoma. *Int. J. Cancer 112*, 1029−1035.
(7) Jiang, A., Gao, X., Zhang, D., Zhang, L., and Lu, H. (2013) Expression and clinical significance of the Trop-2 gene in advanced non-small cell lung carcinoma. *Oncol. Lett. 6*, 375−380.
(8) Fong, D., Moser, P., Krammel, C., Gostner, J. M., Margreiter, R., Mitterer, M., Gastl, G., and Spizzo, G. (2008) High expression of TROP2 correlates with poor prognosis in pancreatic cancer. *Br. J. Cancer 99*, 1290−1295.
(9) Mühlmann, G., Spizzo, G., Gostner, J., Zitt, M., Maier, H., Moser, P., Gastl, G., Zitt, M., Müller, H. M., Margreiter, R., et al. (2009) TROP2 expression as prognostic marker for gastric carcinoma. *J. Clin. Pathol. 62*, 152−158.
(10) Wang, J., Day, R., Dong, Y., Weintraub, S. J., and Michel, L. (2008) Identification of Trop-2 as an oncogene and an attractive therapeutic target in colon cancers. *Mol. Cancer Ther. 7*, 280−285.
(11) Trerotola, M., Cantanelli, P., Guerra, E., Tripaldi, R., Aloisi, A., Bonasera, V., Lattanzio, R., de Lange, R., Weidle, U. H., Piantelli, M., et al. (2013) Upregulation of Trop-2 quantitatively stimulates human cancer growth. *Oncogene 32*, 222−233.
(12) Ripani, E., Sacchetti, A., Corda, D., and Alberti, S. (1998) Human Trop-2 is a tumor-associated calcium signal transducer. *Int. J. Cancer 76*, 671−676.
(13) Stoyanova, T., Goldstein, A. S., Cai, H., Drake, J. M., Huang, J., and Witte, O. N. (2012) Regulated proteolysis of Trop2 drives epithelial hyperplasia and stem cell self-renewal via β-catenin signaling. *Genes Dev. 26*, 2271−2285.
(14) Basu, A., Goldenberg, D. M., and Stein, R. (1995) The epithelial/carcinoma antigen EGP-1, recognized by monoclonal antibody RS7-3G11, is phosphorylated on serine 303. *Int. J. Cancer 62*, 472−479.
(15) Guerra, E., Trerotola, M., Aloisi, A., Tripaldi, R., Vacca, G., La Sorda, R., Lattanzio, R., Piantelli, M., and Alberti, S. (2013) The Trop-2 signalling network in cancer growth. *Oncogene 32*, 1594−1600.
(16) Cubas, R., Zhang, S., Li, M., Chen, C., and Yao, Q. (2010) Trop2 expression contributes to tumor pathogenesis by activating the ERK MAPK pathway. *Mol. Cancer 9*, 253.
(17) Panowski, S., Bhakta, S., Raab, H., Polakis, P., and Junutula, J. R. (2014) Site-specific antibody drug conjugates for cancer therapy. *mAbs 6*, 34−45.
(18) Stein, R., Basu, A., Chen, S., Shih, L. B., and Goldenberg, D. M. (1993) Specificity and properties of Mab RS7-3G11 and the antigen defined by this pancarcinoma monoclonal antibody. *Int. J. Cancer 55*, 938−946.
(19) Stein, R., Basu, A., Goldenberg, D. M., Lloyd, K. O., and Mattes, M. J. (1994) Characterization of cluster 13: the epithelial/carcinoma antigen recognized by Mab RS7. *Int. J. Cancer, Suppl. 8*, 98−102.
(20) Cardillo, T. M., Govindan, S. V., Sharkey, R. M., Trisal, P., and Goldenberg, D. M. (2011) Humanized anti-Trop-2 IgG-SN-38 conjugate for effective treatment of diverse epithelial cancers: Preclinical studies in human cancer xenograft models and monkeys. *Clin. Cancer Res. 17*, 3157−3169.
(21) Shih, L. B., Xuan, H., Aninipot, R., Stein, R., and Goldenberg, D. M. (1995) In vitro and in vivo reactivity of an internalizing antibody, RS7, with human breast cancer. *Cancer Res. 55*, 5857s−5863s.
(22) Junutula, J. R., Flagella, K. M., Graham, R. A., Parsons, K. L., Ha, E., Raab, H., Bhakta, S., Nguyen, R., Dugger, D. L., Li, G., et al. (2010) Engineered thio-trastuzumab−DM1 conjugate with an improved therapeutic index to target human epidermal growth factor receptor 2-positive breast cancer. *Clin. Cancer Res. 16*, 4769−4778.
(23) Goldenberg, D. M., Vahdat, L. T., Starodub, A. N., Bardia, A., Chuang, E., Moroose, R. L., Diamond, J. R., Sharkey, R. M., Maliakal, P. P., Hamburger, S. A., et al. (2014) IMMU-132, a potential new antibody−drug conjugate (ADC) for the treatment of triple-negative breast cancer (TNBC): preclinical and initial clinical results, San Antonio Breast Cancer Symposium, San Antonio, TX, December 9−13, Abstract no. P5-19-08.
(24) Bardia, A., Starodub, A., Moroose, R. L., Mayer, I. A., Diamond, J. R., Chuang, E., Govindan, S. V., Sharkey, R. M., Maliakal, P., Wegner, W. A., et al. (2014) IMMU-132, a new antibody−drug conjugate (ADC) against Trop-2, as a novel therapeutic for patients with relapsed/refractory, metastatic, triple-negative breast cancer (TNBC): results from Phase I/II clinical trial (NCT01631552), San Antonio Breast Cancer Symposium, San Antonio, TX, December 9−13, Abstract no. P5-19-27.
(25) Cusack, J. C., Jr., Liu, R., Houston, M., Abendroth, K., Elliott, P. J., Adams, J., and Baldwin, A. S., Jr. (2001) Enhanced chemosensitivity to CPT-11 with proteasome inhibitor PS-341: implications for systemic nuclear factor-κB inhibition. *Cancer Res. 61*, 3535−3540.
(26) Liu, Y., Xing, H., Weng, D., Song, X., Qin, X., Xia, X., Weng, Y., Liang, F., Chen, G., Han, X., et al. (2008) Inhibition of Akt signaling by SN-38 induces apoptosis in cervical cancer. *Cancer Lett. 274*, 47−53.
(27) Lagadec, P., Griessinger, E., Nawrot, M. P., Fenouille, N., Colosetti, P., Imbert, V., Mari, M., Hofman, P., Czerucka, D., Rousseau, D., et al. (2008) Pharmacological targeting of NF-κB potentiates the effect of the topoisomerase inhibitor CPT-11 on colon cancer cells. *Br. J. Cancer 98*, 335−344.
(28) Whitacre, C. M., Zborowska, E., Willson, J. K. V., and Berger, N. A. (1999) Detection of poly(ADP-ribose) polymerase cleavage in response to treatment with topoisomerase I inhibitors: a potential surrogate end point to assess treatment effectiveness. *Clin. Cancer Res. 5*, 665−672.
(29) Sherr, C. J., and Roberts, J. M. (1995) Inhibitors of mammalian G1 cyclin-dependent kinases. *Genes Dev. 9*, 1149−1163.
(30) Fluda, S., and Debatin, K.-M. (2006) Extrinsic versus intrinsic apoptosis pathways in anticancer chemotherapy. *Oncogene 25*, 4798−4811.
(31) Starodub, A. D., Ocean, A. J., Bardia, A., Guarino, M. J., Messersmith, W., Berlin, J., Picozzi, V. J., Thomas, S. S., Masters, G., Vahdat, L. T., et al. (2015) Advanced solid cancer therapy with a novel antibody−drug conjugate (ADC), sacituzumab govitecan (IMMU-132): key preclinical and clinical results, American Association for Cancer Research (AACR) Annual Meeting, Philadelphia, PA, April 18−22, Abstract no. CT236.
(32) Starodub, A.; Ocean, A. J.; Shah, M. A.; Guarino, M. J.; Picozzi, V. J.; Vahdat, L. T.; Thomas, S. S.; Govindan, S. V.; Maliakal, P. P.; Wegner, W. A. First-in-human trial of a novel anti-Trop-2 antibody-SN-38 conjugate, sacituzumab govitecan, for the treatment of diverse metastatic solid tumors, *Clin. Cancer Res.* 2015, in press.
(33) Sharkey, R. M., McBride, W. J., Cardillo, T. M., Govindan, S. V., Wang, Y., Rossi, E. A., Chang, C.-H., Goldenberg, D. M. (2015) Enhanced delivery of SN-38 to human tumor xenografts with an anti-

DOI: 10.1021/acs.bioconjchem.5b00223
Bioconjugate Chem. 2015, 26, 919−931

Trop-2-SN-38 antibody conjugate (sacituzumab govitecan), submitted for publication.
(34) Picozzi, V. J., Ocean, A. J., Starodub, A. N., Thomas, S. S., Maliakal, P. P., Govindan, S. V., Hamburger, S. A., Sharkey, R. M., and Goldenberg, D. M. (2014) IMMU-132, a new antibody−drug conjugate (ADC), evaluated in patients with advanced, metastatic, pancreatic ductal adenocarcinoma (mPC): results of a Phase I/II trial, American Association for Cancer Research (AACR) Special Conference on Pancreatic Cancer: Innovations in Research and Treatment, New Orleans, LA, May 18−21, Abstract no. B99.
(35) Starodub, A., Ocean, A. J., Guarino, M. J., Picozzi, V. J., Thomas, S. S., Messersmith, W. A., Shah, M. A., Vahdat, L. T., Chuang, E., Lin, B. S. (2014) IMMU-132, an SN-38 antibody−drug conjugate (ADC) targeting Trop-2, as a novel platform for the therapy of diverse metastatic solid cancers: clinical results, American Society of Clinical Oncology (ASCO) Annual Meeting, Chicago, IL, May 30−June 3, Abstract no. 3032
(36) Raji, R., Guzzo, F., Carrara, L., Varughese, J., Cocco, E., Bellone, S., Betti, M., Todeschini, P., Gasparrini, S., Ratner, E., et al. (2011) Uterine and ovarian carcinosarcomas overexpressing Trop-2 are sensitive to hRS7, a humanized anti-Trop-2 antibody. *J. Exp. Clin. Cancer Res. 30*, 106.
(37) Bignotti, E., Ravaggi, A., Romani, C., Falchetti, M., Lonardi, S., Facchetti, F., Pecorelli, S., Varughese, J., Cocco, E., Bellone, S., et al. (2011) Trop-2 overexpression in poorly differentiated endometrial endometrioid carcinoma: implications for immunotherapy with hRS7, a humanized anti-trop-2 monoclonal antibody. *Int. J. Gynecol. Cancer 21*, 1613−1621.
(38) Varughese, J., Cocco, E., Bellone, S., Ratner, E., Silasi, D. A., Azodi, M., Schwartz, P. E., Rutherford, T. J., Buza, N., Pecorelli, S., et al. (2011) Cervical carcinomas overexpress human trophoblast cell-surface marker (Trop-2) and are highly sensitive to immunotherapy with hRS7, a humanized monoclonal anti-Trop-2 antibody. *Am. J. Obstet. Gynecol. 205*, 567.e1−567.e7.
(39) Varughese, J., Cocco, E., Bellone, S., Bellone, M., Todeschini, P., Carrara, L., Schwartz, P. E., Rutherford, T. J., Pecorelli, S., and Santin, A. D. (2011) High-grade, chemotherapy-resistant primary ovarian carcinoma cell lines overexpress human trophoblast cell-surface marker (Trop-2) and are highly sensitive to immunotherapy with hRS7, a humanized monoclonal anti-Trop-2 antibody. *Gynecol. Oncol. 122*, 171−177.
(40) Varughese, J., Cocco, E., Bellone, S., de Leon, M., Bellone, M., Todeschini, P., Schwartz, P. E., Rutherford, T. J., Pecorelli, S., and Santin, A. D. (2011) Uterine serous papillary carcinomas overexpress human trophoblast-cell-surface marker (Trop-2) and are highly sensitive to immunotherapy with hRS7, a humanized anti-Trop-2 monoclonal antibody. *Cancer 117*, 3163−3172.
(41) Bonner, W. M., Redon, C. E., Dickey, J. S., Nakamura, A. J., Sedelnikova, O. A., Solier, S., and Pommier, Y. (2008) GammaH2AX and cancer. *Nat. Rev. Cancer 8*, 957−967.
(42) Junghans, R. P., and Anderson, C. L. (1996) The protection receptor for IgG catabolism is the beta2-microglobulin-containing neonatal intestinal transport receptor. *Proc. Natl. Acad. Sci. U.S.A. 93*, 5512−5516.
(43) Datta-Mannan, A., Witcher, D. R., Tang, Y., Watkins, J., and Wroblewski, V. J. (2007) Monoclonal antibody clearance. Impact of modulating the interaction of IgG with the neonatal Fc receptor. *J. Biol. Chem. 282*, 1709−1717.
(44) Goldenberg, D. M., Cardillo, T. M., Govindan, S. V., Rossi, E. A., Sharkey, R. M. (2015) Trop-2 is a new candidate target for solid cancer therapy with sacituzumab govitecan (IMMU-132), an antibody−drug conjugate (ADC), submitted for publication.
(45) Park, B. W., Zhang, H. T., Wu, C., Berezov, A., Zhang, X., Dua, R., Wang, Q., Kao, G., O'Rourke, D. M., Greene, M. I., et al. (2000) Rationally designed anti-HER2/neu peptide mimetic disables P185HER2/neu tyrosine kinases in vitro and in vivo. *Nat. Biotechnol. 18*, 194−198.
(46) Berezov, A., Zhang, H. T., Greene, M. I., and Murali, R. (2001) Disabling erbB receptors with rationally designed exocyclic mimetics of antibodies: structure−function analysis. *J. Med. Chem. 44*, 2565−2574.
(47) Young, T., Abel, R., Kim, B., Berne, B. J., and Friesner, R. A. (2007) Motifs for molecular recognition exploiting hydrophobic enclosure in protein−ligand binding. *Proc. Natl. Acad. Sci. U.S.A. 104*, 808−813.
(48) Li, Y., Huang, Y., Swaminathan, C. P., Smith-Gill, S. J., and Mariuzza, R. A. (2005) Magnitude of the hydrophobic effect at central versus peripheral sites in protein-protein interfaces. *Structure 13*, 297−307.
(49) Lewis Phillips, G. D., Li, G., Dugger, D. L., Crocker, L. M., Parsons, K. L., Mai, E., Blättler, W. A., Lambert, J. M., Chari, R. V., Lutz, R. J., et al. (2008) Targeting HER2-positive breast cancer with trastuzumab-DM1, an antibody-cytotoxic drug conjugate. *Cancer Res. 68*, 9280−9290.
(50) Erickson, H. K., Lewis Phillips, G. D., Leipold, D. D., Provenzano, C. A., Mai, E., Johnson, H. A., Gunter, B., Audette, C. A., Gupta, M., Pinkas, J., et al. (2012) The effect of different linkers on target cell catabolism and pharmacokinetics/pharmacodynamics of trastuzumab maytansinoid conjugates. *Mol. Cancer Ther. 11*, 1133−1142.
(51) Govindan, S. V., Cardillo, T. M., Sharkey, R. M., Tat, F., Gold, D. V., and Goldenberg, D. M. (2013) Milatuzumab-SN-38 conjugates for the treatment of CD74+ cancers. *Mol. Cancer Ther. 12*, 968−978.
(52) Moon, S.-J., Govindan, S. V., Cardillo, T. M., D'Souza, C. A., Hansen, H. J., and Goldenberg, D. M. (2008) Antibody conjugates of 7-ethyl-10-hydroxycamptothecin (SN-38) for targeted cancer chemotherapy. *J. Med. Chem. 13*, 6916−6926.
(53) Govindan, S. V., Cardillo, T. M., Moon, S.-J., Hansen, H. J., and Goldenberg, D. M. (2009) CEACAM5-targeted therapy of human colonic and pancreatic cancer xenografts with potent labetuzumab−SN-38 immunoconjugates. *Clin. Cancer Res. 15*, 6052−6061.
(54) Wang, W., Lu, P., Fang, Y., Hamuro, L., Pittman, T., Carr, B., Hochman, J., and Prueksaritanont, T. (2011) Monoclonal antibodies with identical Fc sequences can bind to FcRn differentially with pharmacokinetic consequences. *Drug Metab. Dispos. 39*, 1469−1477.

DOI: 10.1021/acs.bioconjchem.5b00223
Bioconjugate Chem. 2015, 26, 919−931